Advances in Computational Design, *Vol. 5, No. 3 (2020) 277-289*
DOI: https://doi.org/10.12989/acd.2020.5.3.277

Finite element modeling of multiplyconnected three-dimensional areas

Askhad M. Polatov*[1], Akhmat M. Ikramov[1] and Daniyarbek D. Razmukhamedov[2]

[1]*Department of Mathematics, National University of Uzbekistan,4, University Street, Tashkent 100174, Uzbekistan*
[2]*Turin Polytechnic University in Tashkent, 17, Kichik halqa yo'li Street, Tashkent 100000, Uzbekistan*

(Received January 18, 2019, Revised November 27, 2019, Accepted December 20, 2019)

Abstract. This article describes the technology for constructing of a multiply-connected three-dimensional area's finite element representation. Representation of finite-element configuration of an area is described by a discrete set that consist of the number of nodes and elements of the finite-element grid, that are orderly set of nodes' coordinates and numbers of finite elements. Corresponding theorems are given, to prove the correctness of the solution method. The adequacy of multiply-connected area topology's finite element model is shown. The merging of subareas is based on the criterion of boundary nodes' coincidence by establishing a simple hierarchy of volumes, surfaces, lines and points. Renumbering nodes is carried out by the frontal method, where nodes located on the outer edges of the structure are used as the initial front.

Keywords: modeling; finite element; grid; numbering; ordering; node; vertex; face; front; algorithm; connect; area

1. Introduction

Carrying out computational experiments based on the finite element method requires automating of the finite element mesh constructing process of a real object. If at the same time the object has a complex configuration, then the construction of a finite element mesh becomes a time consuming process.

A common approach for generating an anisotropic mesh is the M-uniform mesh approach where an adaptive mesh is generated as a uniform one in the metric specified by a given tensor M. A key component is the determination of an appropriate metric which is often based on some type of Hessian recovery. Kamenski (Kamenski 2011) discusses the usage of this method for a selection of different applications. Numerical results show that the method performs well and is comparable with existing metric tensors based on Hessian recovery. Also, it can provide even better adaptation to the solution if applied to problems with gradient jumps and steep boundary layers. For the Poisson problem in a domain with a corner singularity, the new method provides meshes that are fully comparable to the theoretically optimal meshes. In paper (Diamond-Kite 2012) family of quadrilateral meshes, that can be adapted to a local size function by local subdivision operations

*Corresponding author, Professor, Ph.D., E-mail: asad3@yandex.ru

http://www.techno-press.org/?journal=acd&subpage=7 ISSN: 2383-8477 (Print), 2466-0523 (Online)

are described. Meshes use a number of elements that is within a constant factor of the minimum possible for any mesh of bounded aspect ratio elements, graded by the same local size function, and is invariant under Laplacian smoothing. The vertices of meshes form the centers of the circles in a pair of dual circle packing's. The same vertex placement algorithm but a different mesh topology gives a pair of dual well-centered meshes adapted to the given size function. The book (Daniel Lo 2015) provides a concise and comprehensive guide to the application of finite element mesh generation over 2D domains, curved surfaces, and 3D space. Organized according to the geometry and dimension of the problem domains, it develops from the basic meshing algorithms to the most advanced schemes to deal with problems with specific requirements such as boundary conformity, adaptive and anisotropic elements, shape qualities, and mesh optimization. In finite element analysis, mesh density is a critical issue which closely relates to the accuracy of the finite element models while directly determines their complexity level. In paper (Liu and Glass 2013) a systematic study on finding the effects of mesh density on the accuracy of numerical analysis results, based on which brief guidelines of choosing the best mesh strategy in finite element modeling are provided. Static, modal, and impact analysis are involved in this study to discuss the effects of element size in finite element analysis. In paper (Pavarino *et al*. 2013), alternatives to solid modeling and automatic generation of highly refined tetrahedral meshes, with quality compatible with other studies focused on mesh generation are demonstrated. Aiming at the bottleneck problem of time and memory in large-scale serial mesh generation, in paper (Wang and Jin 2014) a method for large-scale parallel unstructured tetrahedral mesh generation is presented. The proposed boundary judgments method based on the shared element was used to solve the matching problem of the partition boundary nodes. Examples illustrating the efficiency and applicability of this method were presented and the examples showed that mesh generation method can get a good efficiency and a high quality tetrahedral mesh. In paper (Zhang *et al*. 2017), the 3D numerical modeling investigation of dam-break flow hydrodynamics in an open L-shape channel has been presented. A newly developed 3D unstructured mesh finite element model is used here. This study shows that the 3D unstructured mesh model is capable of capturing the 3D hydraulic aspects and complicated local flows around structures in simulation of dam-break flows. In this paper (Pochet *et al*. 2017) a new method for adaptive all-quadrilateral mesh generation for two-dimensional domains, including domains modeled by constraints with complex geometry or with varying scales is presented. The method subdivides the domain's bounding box using a new extended quadtree scheme. In this subdivision process, the quadtree node corners are moved onto the geometrical constraints using local deformation criteria during the tree refinement steps. During the process, grid alignment with constraint accuracy and element quality at every scale is ensuring. Results showed that method generates elements of reasonable quality even for complex geometries and varying scales. The small number of parameters controlling the process is intuitive and makes method efficient and user friendly. The presence of a few inverted or poor-quality mesh elements can negatively affect the stability, convergence and efficiency of a finite element solver and the accuracy of the associated partial differential equation solution. In paper (Sastry *et al*. 2014) a mesh quality improvement and untangling method that untangles a mesh with inverted elements and improves its quality is proposed. The method uses a logarithmic barrier function and performs global mesh quality improvement. Also developed a smooth quality metric that takes both signed area and the shape of an element into account. This quality metric assigns a negative value to an inverted element. It is used to untangle a mesh by improving the quality of an inverted element to a positive value. Method yields better quality meshes than existing methods for improvement of the worst quality elements, such as the active set, pattern search, and

multidirectional search mesh quality improvement methods. Adaptive meshing of 2D planar regions, curved surfaces as well as 3D volumes has been extensively studied in finite element analyses of heterogeneous objects. The approach proposed in the paper of (You *et al*. 2015) takes full advantages of the material heterogeneity information and the mesh density is formulated with a specific function of the material variations. Dual triangulation of centroid Voronoi tessellation is then constructed and necessary mesh subdivision is applied with respect to a predefined material threshold. Results analysis show that the proposed method can significantly decrease the mesh complexities as well as computational resources in FEA of heterogeneous objects.

In many engineering Computational Fluid Dynamics (CFD) applications, the computational domain changes with time due to the movement of boundaries. In paper (Zheng *et al*. 2020) dynamic numerical method was developed to predict the growth of ash deposit on the deposition probe. Based on the CFD dynamic mesh technique, both shape variations and surface temperature variations of ash deposit with time were predicted. Adaptive remeshing technique that works with any element shape and geometry where the mesh adapts to each scan vector was developed in (Olleak and Xi 2018). In paper (Olleak and Xi 2019), mesh adaptively proposed in authors' previous paper (Olleak and Xi 2018) was extended to part-level simulation with FE modeling to reduce the computational time without sacrificing the accuracy. The objective is to handle large domain simulations along with high computational efficiency. The influence of crack tip angle on fracture mechanics parameters is investigated in paper (Branco *et al*. 2015) by extending the crack using defined increments is such a way that intergranular deviations are modeled. The level of accuracy and scatter in the data from experimental testing and numerical modeling helps to determine the confidence of the life assessments calculations. For this purpose a novel method of meshing which replicates a polycrystalline grain structure is developed. In paper (Yang *et al*. 2015) introduces a mesh generation strategy devised and implemented for the volume element model, and elaborates key contributions of the strategy in enhancing the volume element model as a prominent tool in ship thermal modeling and simulation. The volume element model mesh generation strategy employs ray crossings and ray–triangle intersection algorithms and constructs sufficiently accurate geometric representations of the whole ship within permissible time frame using hexahedral meshes.

The book (Piegl and Tiller 1996) covers all aspects of non-uniform rational B-splines necessary to design geometry in a computer aided environment. Basic B-spline features, curve and surface algorithms, and state-of-the-art geometry tools are all discussed. Detailed code for design algorithms and computational tricks are covered too, in a lucid, easy-to-understand style.

This paper describes the technology for constructing a finite element representation of a multiplyconnected three-dimensional area. The finite-element representation of the configuration of an area is described by a discrete set consisting of the number of nodes and finite elements of the finite-element grid, ordered sets of coordinates of nodes and node numbers by finite elements. To prove the correctness of the solution method, the corresponding theorems are given, where the adequacy of a finite element model of the topology of a multiply connected area is proved. The algorithm of method includes the following steps:

- formation of a finite element mesh of elementary subareas;
- stitching (combining) subareas;
- the formation of a set of initial fronts;
- ordering the node numbers of the finite element model;
- minimization of the tape width of the system of equations.

The merging of subareas is based on the criterion of coincidence of boundary nodes by

establishing a simple hierarchy of volumes, surfaces, lines and points. The formation of elements of the set of initial fronts is carried out by determining the numbers of vertices and boundary nodes of the finite element representation of multiplyconnected areas. Renumbering nodes and finite elements is carried out on the basis of the front method. As nodes of the initial front, a set of nodes are used, this is located on edge of the construction.

2. Description of the method for solving the problem

The finite element mesh of a complex object is formed by stitching elementary subareas. By elementary is meant the area for which there is an algorithm for constructing a finite element mesh. A quadrilateral (in the case of a two-dimensional body) or a quadrangular prism (for a three-dimensional body) is used as the shape of the finite elements, since filling the real area with these elements is very effective.

The following introduce definitions and the criterion for the coincidence of the boundary nodes of the representation sets.

Definition 1. The topology of a complex area model is called:

1) a one-dimensional area represented by a system of interconnected linear elements intersecting at the nodal points; however, each of them may have several intermediate nodes;

2) a two-dimensional area represented by a system of interconnected surfaces, adjoining along boundary lines intersecting at nodal points; however, the boundary lines may also include a number of intermediate nodes; surfaces may be limited by several lines; two lines must be connected so that one of them intersects the other at the end point;

3) a three-dimensional area represented by a system of interconnected volume elements bounded by surfaces intersecting at nodal points; boundary surfaces and lines, as well as each volume element, can have some number of internal nodes; surfaces can intersect only along boundary lines.

Thus, a simple hierarchy of volumes, surfaces, lines and points is established.

Definition 2. In the decomposition, a multiply-connected area is divided into a number of elementary subareas, and the corresponding boundary surfaces of adjacent subareas have the same configuration.

For each of the configurations of the elementary subareas' surface, its own method of splitting into finite elements is used.

When merging subareas, the partitioning parameters of the boundary stitching surfaces are set identical, this ensures the coincidence of the coordinates of the nodes on the surface of the union of adjacent subareas.

Definition 3. A finite-element representation of an area configuration is a discrete set:

$$\Omega = \{n, m, K, M\}, \tag{1}$$

where

n - is the number of nodes of the finite element mesh;

m- is the number of finite elements;

K - is the ordered set of coordinates of nodes;

M - is an ordered set of node numbers by finite elements.

Criterion. The condition for the coincidence of the boundary nodes of the two sets Ω_1 and Ω_2 is the relation

$$\left|x_i^1 - x_j^1\right| < \varepsilon \,\&\, \left|x_i^2 - x_j^2\right| < \varepsilon \,\&\, \left|x_i^3 - x_j^3\right| < \varepsilon, \tag{2}$$

where

$(x_i^1, x_i^2, x_i^3) \in K_1$ - is the set of coordinates of nodes Ω_1 (i = 1, 2, ... , n_1);

$(x_j^1, x_j^2, x_j^3) \in K_2$ - is the set of coordinates of nodes Ω_2 (j = 1, 2, ... , n_2);

$\varepsilon > 0$ - is a sufficiently small number.

Based on the above definitions and criteria, the following theorems are proved.

Theorem 1. Suppose that when combining the sets $\Omega_1 = \{n_1, m_1, K_1, M_1\}$ and $\Omega_2 = \{n_2, m_2, K_2, M_2\}$, the conditions of the topology of a doubly connected area model (definition 1 and 2) are satisfied, then

$$m = m_1 + m_2, \quad n = n_1 + n_2 - q, \tag{3}$$

where

m, n - is the total number of finite elements and nodes, respectively;

$q=|K_1 \cap K_2|$ - the number of identifiable (ε-nearby) nodes located on the boundary of the compound of subareas;

K_1, K_2 – are ordered sets of nodes coordinates.

Evidence. Since the two subareas are combined by boundary nodal points, the total number of finite elements is equal to their sum, i.e. $m=m_1+m_2$. According to definition 2, when combining two subareas intersecting at boundary nodes, the nodes coincide. In this case, the total number of nodes:

$$n = n_1 + n_2 - q, \tag{4}$$

where q- is the number of coincident boundary nodes, which is determined by the criterion. The fulfillment of the criterion means that the boundary nodes coincide up to a sufficiently small value of $\varepsilon > 0$. ■

Theorem 2. Suppose that unification of the sets $\Omega_1 = \{n_1, m_1, K_1, M_1\}$ and $\Omega_2 = \{n_2, m_2, K_2, M_2\}$ satisfies the conditions of the topology of the model of a doubly connected area (definition 1 and 2), then

$$M = M_1 \cup M_2', \quad K = K_1 \cup K_2', \tag{5}$$

where,

K_2'- is an ordered set of coordinates of the nodes of the set Ω_2 without considering the boundary nodes that coincide with the boundary nodes of the set $K_1 \subset \Omega_1$;

M_2'- an ordered set of the numbered nodes of the set $M_2 \subset \Omega_2$.

Evidence. According to Theorem 1, $m=m_1+m_2$, $n=n_1+n_2-q$.

For the numbering of local node numbers of the sets Ω_1 and Ω_2, respectively, the sets are introduced:

$$N_1 = \{ i \mid i \le n_1 \}, \quad i \in N \qquad \text{and} \qquad N_2 = \{ j \mid j \le n_2 \}, \quad j \in N. \tag{6}$$

Next, sets are introduced: A and B ($|A|=|B|=q$). The elements of these sets are the local numbers of the coinciding boundary nodes, respectively, from the sets of nodes N_1 and N_2, which satisfy the relation of the Cartesian product of sets:

$$\mathrm{A} \times \mathrm{B} = \left\{ (i, j) \mid i \in N_1,\ j \in N_2 : \sum_{k=1}^{l} \left| x_i^k - x_j^k \right| < l\varepsilon \right\}, \tag{7}$$

where, $\varepsilon \succ 0$ – is a sufficiently small number; $l = 3$

The formation of elements of a set of node numbers by finite elements M includes the following steps:

1) the initial k=1,2,…,m_1 elements of the set M are assigned the elements of the set M_1, i.e. $M_1 \subset M$;

2) the next k=m_1+1, m_1+2,…,m_1+ m_2 elements of the set M are formed by replacing the local numbers of the nodes of the set M_2 with global numbers, i.e. $M = M_1 \cup M_2'$, where is a set consisting of global node numbers. The process of global node numbers' calculation is carried out according to the following rule. If the local node number i of the set N_2(i=1,2,…,n_2) belongs to the set-B, i.e. $i \in B$, then it is assigned the corresponding local node number from the set-A. In the opposite case, its value is calculated based on the ratio $i' \to i+n_1-z$, where the value of the variable z is defined as the number of elements of the set B whose values are less than the current number i, those

$$z = |Q(i;B)|, \tag{8}$$

where

$$Q(i;B) = \{ j \in B : j \prec i \}. \tag{9}$$

The formation of elements of the set of coordinates of nodes K consists of the following steps:

1) the initial k=1,2,…,n_1 elements of the set K are assigned the elements of the set K_1 , i.e. $K_1 \subset K$;

2) the subsequent $k = n_1 + 1, n_1 + 2, ..., n_1 + n_2 - q$ elements of the set K are formed from the elements of the subset K_2 without considering the numbers of nodes in the set B, i.e.

$$K = K_1 \bigcup K_2', \text{ where } K_2' \subset K_2 \quad \text{and} \quad |K_2'| = n_2 - q. \tag{10}$$

Thus, all components of the set Ω- of a finite element representation of the original doubly connected area are defined. ■

Theorems 1 and 2 can be generalized by the following theorem.

Theorem 3. Suppose that for the sets Ω_i (i=1,2,…,p) the conditions of the topology of the model of a complex area (Definition 1 and 2) are fulfilled. Then for the multiply connected area Ω, the following relation holds:

$$\Omega = \bigcup_{i=1}^{p} \Omega_i \tag{11}$$

where $p-$ is the number of subareas to be combined.

Evidence. When p=2, according to Theorems 1 and 2, relation (11) holds. Next, using the principle of mathematical induction, we assume that relation (11) is true for p–1, i.e.

$$\Omega^{p-1} = \bigcup_{i=1}^{p-1} \Omega_i \,. \tag{12}$$

Then for the multiply-connected domain Ω, the following relation holds:

$$\Omega = \Omega^{p-1} \cup \Omega_p \,. \tag{13}$$

According to Theorems 1 and 2, relation (13) is also satisfied. ■

Thus, the mathematical correctness of the algorithm for constructing a finite-element topology of a multiplyconnected area is proved.

3. The technology of constructing a finite element meshes of a multiplyconnected area

Based on the above theorems, the technology for constructing a finite element mesh of a multiplyconnected area has been developed, the algorithm of which includes the following steps:

1) partition of the original body into elementary subareas;
2) the union of subareas;
3) the definition of the initial fronts;
4) ordering the node numbers of the finite element model;
5) minimization of tape width of the system of equations.

Consider each of these stages separately.

3.1 The technology of dividing the construction into elementary subareas

It is known that when the construction is deformed near the structural features (cavity, recess, etc.) of the simulated structure, elevated stresses are observed. In this connection, the discretization of the hub neighborhood is performed with a compacted finite element mesh, and the rest of the body part - is a uniformly distributed mesh.

When splitting the original body into elementary subareas, first of all, areas located near structural features are distinguished, and the remaining part – is filled with elementary subareas with a uniform grid (see calculation examples 1 and 2 in Section 4 and Section 5, respectively).

3.2 The method of combining elementary subareas

The procedure for combining elementary areas includes the following steps:

1) on the basis of a comparison of the coordinates of nodes located in arrays K_1 and K_2, they form:

– the number of nodes located on the border of the union of the areas;

– arrays A and B, which consist of numbers of coincident nodes, respectively, of the sets Ω_1 and Ω_2;

2) the values of the elements of the array M_1 are the initial elements of the array M;

3) the subsequent values of the elements of the array M are formed by replacing the local node numbers of the set Ω_2 located in the array M_2 with global numbers. If the value of the current i-th node number located in array N_2 is present in array B, then the i-th node is assigned the corresponding local node number from array A. Otherwise, its current value is calculated based on the ratio: $i' \rightarrow i+n_1-z$, where the value of the variable z is defined as a number, which is defined as the number of nodes in the N_2 array, whose numbers are less than the value of i. In a corresponding way (Theorem 2), the elements of an array of coordinates of nodes - K are formed.

It should be noted that the elements K and M of the set Ω have dimensions:

$$K \quad [1 \div \mathrm{n},\ 1 \div \mathrm{n}v] \text{ and } \quad M \quad [1 \div \mathrm{m},\ 1 \div \mathrm{n}u],$$

where

nv - is the dimension of the space;

nu - is the number of nodes in the final element.

3.3 Algorithm for determining the initial front

The method of determining the initial fronts consider the example of a multiplyconnected two-dimensional area. The best results are obtained when choosing as the initial fronts of an ordered set of nodes located on the edges and vertices of the finite element mesh of a multiplyconnected area. In this connection, we introduce the corresponding definitions (Polatov and Fedorov 2007).

The ***vertex*** in the finite element representation of a multiplyconnected domain is a node that occurs in only one finite element.

Boundary nodes are nodes located on the border of an area or on the boundary between two vertices.

The process of finding boundary nodes is as follows:

1) randomly select a node that meet in two finite elements, and is added to the front;

2) the process of searching for nodes that occur only once in two finite elements, which are described in clause 1, is carried out. If there are none, then in the initial front, a search is repeated for nodes that occur twice. Otherwise, the formation of the initial front ends. Then the front is cleared and the transition to point 1 is carried out, otherwise the number of this node is added to the front;

3) if in the process of repeated execution of the described actions in the second step a vertex is found twice, then the search for the edge is completed and the front ordering is performed;

4) all nodes occurring once or twice are added to the front and the actions described in clauses 2-3 are performed;

5) steps 1-4 are repeated until all edges between two vertices are found.

To prevent this process from looping, all nodes found in two finite elements should be “tagged” and not used in the future. The remaining vertices or edges can be found by replacing the condition in the third paragraph, i.e. exit from the loop occurs if a “tagged” node is found.

3.4 Modified frontal node renumbering method

For the ordering procedure for node numbers, three fronts are used: in the first one, the node numbers of the initial or current front are located, in the second, the numbers of the nodes of the previous one, and in the third, the number of nodes of the appearance new front.

The algorithm of the modified frontal method consists of the following steps:

1) vertices or boundary nodes are selected as the source front;

2) finite elements that contain node numbers that coincide with the numbers of front nodes will be determined;

3) the node numbers selected in step 2 that are involved in the current, previous and in the forming fronts will be excluded;

4) according to the following rule, the grid nodes that have a number that are identical with the numbers of nodes in the current front are renumbered. Each next numbered node gets a number one greater than the previous one. The most initial renumbered node is number one;

5) the contents of the current front are saved (now it becomes the previous one). The contents of the newly formed front are copied into the current one with its subsequent purification. Those, the front "moves" on a finite element mesh;

6) all the actions described in clauses 2-5 are repeated until the formed front is empty.

3.5 The method of minimizing the width of the tape system of equations

The final stage of the method is the ordering of the numbers of nodes and finite elements of the finite element of representation, which allows minimizing the width of the tape of resolving equations (Sakovich and Kholmyansky 1981, George and Liu 1984). For this purpose, the frontal procedure is performed for each initial front (Kamel and Eisenstein 1974). For each finite element $i\,(i=1,2,...,m),$ the difference between the maximum and minimum node numbers is calculated:

$$h_i = n_{\max} - n_{\min}\,. \tag{14}$$

Then, by the ratio

$$l_k = \left(\max_{1\le i\le m} h_i + 1 \right) \times V\,, \tag{15}$$

the half width of the tape of the resolving system of equations corresponding to the given initial front is calculated, here V - is the dimension of the space, k- is the current index of the initial fronts.

The minimum value of L is calculated as

$$L = \min_{1\le k\le q} l_k\,, \tag{16}$$

where,

q- is the number of initial fronts.

Since for any construction the number of vertices, edges and side surfaces is limited, the number of searches q is also limited.

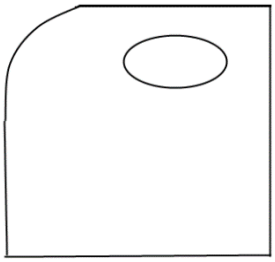

Fig.1 Source area

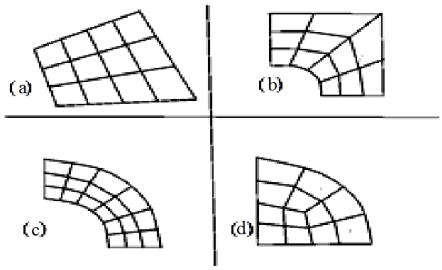

Figs. 2 Forms of elementary subareas

4. Example of calculation 1

For clarity, the process of forming a finite element mesh of a two-dimensional area of complex configuration (Fig. 1) is considered.

The following subareas are used as elementary areas (Figs. 2):

(a) – an arbitrary quadrilateral;

(b) – a rectangle with an elliptic notch at the top;

(c) – 1⁄4 part of the torus;

(d) – 1⁄4 part of the ellipse.

The initial data for the finite element mesh of these subareas are:

(a) - the coordinates of the vertices, the number of partitions along the axes of the OX and OY;
(b) - the coordinates of the center and the radii of the ellipse, the dimensions of the sides of the rectangle, the number of radial partitions and the number of divisions along the OX axis;

(c) - coordinates of the center and radii of the ellipse, the number of radial partitions and the number of divisions along the OX axis;

(d) - the coordinates of the center and the radii of the ellipse, the number of parts along the axes OX and OY.

Taking into account the configuration, the studied area is divided into elementary similar areas (Fig. 3(a)). The area in the upper left corner is replaced by an elementary area in the shape of 1/4 parts of the ellipse. To do this, first remove the rectangular area. Then, instead of it, the necessary area is inserted with the configuration corresponding to the source area. The rectangular area located in the upper right corner is replaced by a rectangle-shaped area with a cavity in the center. The area is formed by the union of four elementary areas in the form of a rectangle with an elliptical notch at the top.

The lower left rectangle is replaced with an elementary area in the shape of 1⁄4 parts of the ellipse. The remaining area, located in the lower right corner, remains unchanged, since its configuration corresponds to the configuration of the source area (Fig. 3(b)).

Forming an area of complex configuration through the usage of a set of elementary subareas allows us to simplify the process of building a finite element mesh by reducing the amount of input source data. The construction algorithm is reduced to the determination of the initial elementary area and the sequence of actions associated with the union of all elementary subareas.
The described method for constructing a finite element mesh of a complex configuration area allows, without increasing the number of finite elements and the number of nodes, to take into account all the geometric features of the area configuration.

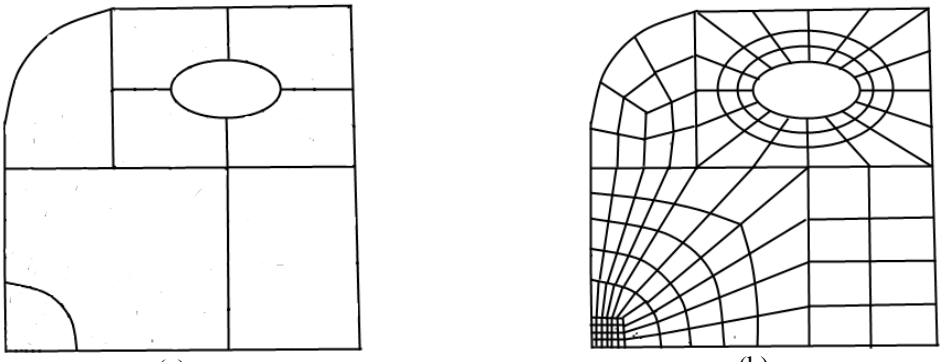

(a) (b)

Figs. 3 The process of composition of a discrete model of complex configuration

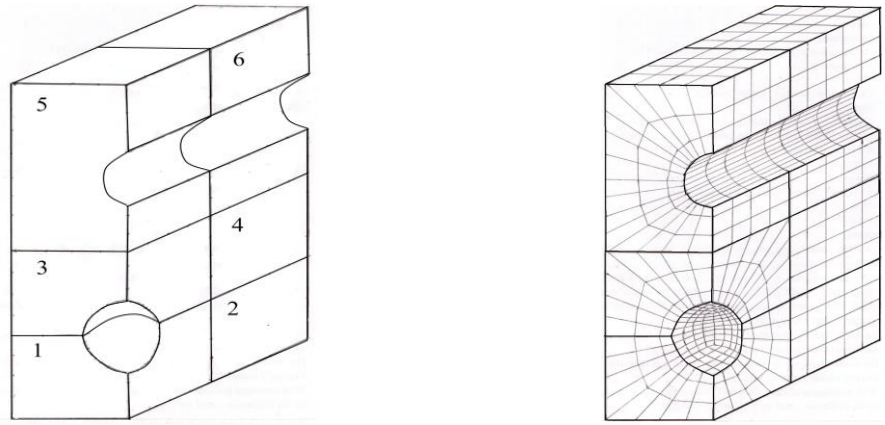

(a) (b)

Figs.4 An example of discretization of a three-dimensional area (only boundary (visible) nodes are shown)

5. Example of calculation 2

To illustrate the process of splitting and discretization of the original body, we consider the process of constructing a finite element representation of a three-dimensional structure in the form of 1/4 of a prism with a spherical cavity and a cylindrical hole. The area is divided into finite elements in the form of quadrilateral prisms. The source area is divided into 6 subareas of the form (Fig. 4(a)):

1 - rectangular prism;

2 - rectangular prism with a spherical notch at the apex;

3 - rectangular prism with a lateral cylindrical recess.

Discretization of the area is shown in Fig. 4(b).

When combining subdomains, the total number of finite elements is summed. The total value of the nodes decreases due to the crosslinking nodes, which are located in the area of crosslinking of the subareas. Table 1 provides information on the process of combining subareas. Parameters are indicated: the type of subdomains, the number of finite elements and nodes in the subdomains, the number of nodes on the stitching surface, the current number of nodes, and their total number.

Table 1 Information on the process of combining subareas

№	number of subareas	number of elements	number of nodes	number of knots stitching	current number of nodes
1	2	144	244	–	244
2	1	80	150	25	125
3	2	144	244	36	208
4	1	80	150	50	100
5	3	192	340	25	315
6	3	240	408	93	315
total		**880**	**1536**	**229**	**1307**

6. Conclusion

The technology of the finite element representation of a multiply-connected three-dimensional area has been developed. It allows the structures to be divided into smaller finite elements of the neighborhood of various kinds of inclusions. This fully reflects the physical essence of the process of deformation of structures.

Acknowledgements

The authors would like to express their appreciations to the administration of National University of Uzbekistan for their financial and overall support and assistance in software package development. The authors also express their appreciation to Prof. Kurmanbaev B. for valuable advices given during analysis of the calculation results. We also acknowledge the valuable assistance of Associate Prof. Gaynazarov S. with computational experiments, of Associate Prof. N. Kadirova for the preparation of articles for publication, F. Polatov, M.Sc., for article translation and edition.

References

Pochet, A., Celes, W., Lopes, H. and Gattass, M. (2017), "A new quadtree-based approach for automatic quadrilateral mesh generation", *Eng. Comput*., **33**(2), 275-292.

Branco, R., Antunes, F.V. and Costa, J.D. (2015), "A review on 3D-FE adaptive remeshing techniques for crack growth modeling", *Eng. Fracture Mech.,* **141**, 170-195.

Daniel Lo, S.H. (2015), *Finite Element Mesh Generation,* CRC Press, Florida, USA. 672.

Eppstein, D. (2012), "Diamond-Kite Adaptive quadrilateral meshing", *Eng. Comput*., **30**(2), 223-225.

Pavarino, E., Neves, L.A., Machado, J.M., de Godoy, M.F., Shiyou, Y., Momente, J.C., Zafalon, G.F., Pinto, A.R. and Valêncio, C.R. (2013), "Tools and strategies for the generation of 3D finite element meshes: Modeling of the cardiac structures", *Int. J. Biomedical Imaging*. https://doi.org/10.1155/2013/540571.

George, A.A. and Liu, J. (1984), *Numerical Solution of Large Sparse Systems of Equations*, Moscow, Russia. 333.

Kamel, X.A. and Eisenstein, G.K. (1974), "Automatic grid generation in two-and three-dimensional composite areas", *High speed computing of Elastic Structures*, *Russia*, *Leningrad*, *Shipbuilding*, (**2**), 21-35. (in Russian).

Kamenski, L. (2011), "A study on using hierarchical basis error estimates in anisotropic mesh adaptation for the finite element method", *Eng. Comput.*, **28**(4), 451-460. https://doi.org/10.1007/s00366-011-0240-z.

Olleak, A. and Xi, Z. (2018), "Finite Element Modeling of the Selective Laser Melting Process for Ti-6Al-4V", *Solid Freeform Fabrication 2018: Proceedings of the 29th Annual International*, Austin, Texas, USA. 1710–1720.

Olleak, A. and Xi, Z. (2019), "Simulation of layer-by-layer selective laser melting process with an efficient remeshing technique", *Procedia Manufact.,* **34**, 613-618. https://doi.org/10.1016/j.promfg.2019.06.167.

Piegl, L. and Tiller, W. (1996), *The NURBS Book*, Springer, Germany.

Polatov, A.M. and Fedorov, A.Yu. (2007), "Algorithm of minimizing the width of the tape of the system of equations", *Modern Information Technologies in Science, Education and Practice*, Orenburg, Russia. 103-105. (in Russian).

Sakovich, A.I. and Kholmyansky, I.A. (1981), "Minimizing the tape width of a system of equations in the finite element method", *Problems of Strength*, **1**, 120-122. (in Russian).

Sastry, S.P., Shontz, S.M. and Vavasis, S.A. (2014), "A log-barrier method for mesh quality improvement and untangling", *Eng. Comput.*, **30**(3), 315-329. https://doi.org/10.1007/s00366-012-0294-6.

Zhang, T., Fang, F. and Feng, P. (2017), "Simulation of dam/levee-break hydrodynamics with a three-dimensional implicit unstructured-mesh finite element model", *Environ. Fluid Mech.*, **17**(5), 959-979. https://doi.org/10.1007/s10652-017-9530-3.

Wang, X.Q. and Jin, X.L. (2014), "A method for large-scale parallel tetrahedral mesh generation", *J. Vib. Shock*, **33**(21), 102-107.

Yang, S., Dilay, E., Ordonez, J.C., Vargas, J.V.C. and Chalfant, J. (2015), "Volume element model mesh generation strategy and its application in ship thermal analysis", *Adv. Eng. Software,* **90**, 107-118. https://doi.org/10.1016/j.advengsoft.2015.08.003.

You, Y.H., Kou, X.Y. and Tan, S.T. (2015), "Adaptive meshing for finite element analysis of heterogeneous materials", *Comput. Aided Design*, **62**, 176-189. https://doi.org/10.1016/j.cad.2014.11.011.

Liu, Y. and Glass, G. (2013), "Effects of mesh density on finite element analysis", *Conference SAE world congress: SAE Technical Papers,* Detroit, Michigan, USA. https://doi.org/10.4271/2013-01-1375.

Zheng, Z., Yang, W., Yu, P. and Cai, Y. and Subbaiah, P. (2020), "Simulating growth of ash deposit in boiler heat exchanger tube based on CFD dynamic mesh technique", *Fuel*, **259**, 116083. https://doi.org/10.1016/j.fuel.2019.116083.

CC